Biophysical Journal, Volume *111*

Supplemental Information

Ultraslow Water-Mediated Transmembrane Interactions Regulate the Activation of A_{2A} Adenosine Receptor

Yoonji Lee, Songmi Kim, Sun Choi, and Changbong Hyeon

SUPPORTING INFORMATION

Details of multiexponential fit of the autocorrelation function of water in Fig. 3. $C(t)$s of water around the residues given in Fig. 3B are fitted to tri-expoential function as follows: $C^{N24}(t) = 0.656e^{-t/1.883\text{ ns}} + 0.047e^{-t/9.453\text{ ns}} + 0.296e^{-t/9.464\text{ ns}}$; $C^{D52}(t) = 0.331e^{-t/0.128\text{ ns}} + 0.349e^{-t/0.790\text{ ns}} + 0.320e^{-t/5.005\text{ ns}}$; $C^{W129}(t) = 0.079e^{-t/0.016\text{ ns}} + 0.021e^{-t/44.108\text{ ns}} + 0.900e^{-t/499.998\text{ ns}}$; $C^{N285}(t) = 0.108e^{-t/0.319\text{ ns}} + 0.438e^{-t/2.365\text{ ns}} + 0.454e^{-t/12.546\text{ ns}}$; $C^{P286}(t) = 0.001e^{-t/0.001\text{ ns}} + 0.085e^{-t/0.182\text{ ns}} + 0.915e^{-t/15.547\text{ ns}}$; $C^{Y288}(t) = 0.852e^{-t/0.199\text{ ns}} + 0.104e^{-t/1.082\text{ ns}} + 0.044e^{-t/4.677\text{ ns}}$, and the average relaxation time of water is obtained by using $\tau = \int_0^\infty C(t)dt$.

Number fluctuation of water molecules on the receptor surfaces. Water undergoes sharp transition from the bulk to interface. Heterogeneity of biomolecular surfaces and conformational dynamics give rise to a number of different classes of interfacial water (1–4). Tempo-spatial variation in the water number and its fluctuation on the receptor surfaces can provide glimpses of the water motion at the interfaces. Some regions of the receptor are persistently occupied by water molecules with small number fluctation, and others with large fluctuation. To quantify the water fluctuation, we counted the number of water molecules as a function of time, $n(t)$, around each residue, and calculated their average ($\langle n\rangle$) and variance ($\langle(\delta n)^2\rangle$) (Fig. S2). As expected, both $\langle n\rangle$ and $\langle(\delta n)^2\rangle$ are larger around the loop regions (ICLs and ECLs) than near the TM helices (see Fig. S2). Taking the ratio between the two numbers, $\langle n\rangle$ and $\langle(\delta n)^2\rangle$, i.e., $F = \langle\delta n^2\rangle/\langle n\rangle$ (Fano factor), one can appraise the influence of the receptor surface on water number fluctuation (Fig. S2).

In calculation, we counted the number of water molecules (n) within 4 Å from any heavy atom of each amino acid residue. Using our 1.2 μsec simulations, we calculated the average number of water ($\langle n\rangle$), variance ($\langle(\delta n)^2\rangle = \langle n^2\rangle - \langle n\rangle^2$), and the ratio between the twos, i.e., Fano factor $F = \langle\delta n^2\rangle/\langle n\rangle$. Residues with suppressed water fluctuations ($F \ll 1$) are commonly found in the ICLs and ECLs of all the three receptor states, and especially in the central zone of TM domain of apo and agonist-bound forms. Notably, the region where the water cluster is detected (Fig. 1B, middle) is surrounded by the residues with $F \ll 1$ (Fig. S2B, black arrows in the bottom panel). Most of the residues with enhanced water fluctuations ($F > 2$) are found at the interface between the receptor and lipid bilayer, especially in TM1, 2, 5, and helix 8. The apo and agonist-bound forms have residues in the TM region with $F < 0.25$, suggestive of strong attractive interactions from TM residues, whereas the TM region of the antagonist-bound form (Fig. S2C) is devoid of such residues.

Internal waters trapped inside the receptor. Among the water molecules that show slow dynamics, some molecules are trapped inside the receptor and tightly bound to specific sites. Tracing the position of the entire water molecules along the trajectories, we systematically identified the trapped water molecules. We divided the full trajectory of 1.2 μs to six intervals (i.e., every 200 ns) and calculated the RMSD of each water oxygen relative to the position in the final snapshot of each interval. Since the average RMSD of trapped water is smaller than that of untrapped free water (≈ 66 Å), it is not difficult to identify the trapped water molecules.

The apo form has two such positions (P_1^{apo} and P_2^{apo} in Fig. S5A). In P_1^{apo}, a water molecule is trapped via tight H-bondings with W129 and S47 during the entire simulation time (1.2 μs) (Fig. S6A). In case of P_2^{apo}, maintaining the H-bonds with Y197, L95, and A99, three water molecules alternate to be trapped (see the three plateau regions in the graph plotting the distances between P_2^{apo} and three water molecules in Fig. S5A). That is, one water molecule in the site is displaced by another water (Supporting Movie M4). Among the residues interacting with the trapped waters, W129$^{4.50}$ and Y197$^{5.58}$ residues are the microswitches.

In the agonist-bound form, trapped waters were observed in three positions (Fig. S5B): The water molecules bound in P_1^{ago} form the H-bonding interactions with N24$^{1.50}$, V282, and F286, connecting the TM1 and TM7 helices. In fact, P_1^{ago} site corresponds to the position where the water cluster with high density is identified in the water density map (Fig. 1B, middle); The water in P_2^{ago} interacts with C245, L249, and A273, mediating the interaction between the TM6 and TM7; Two water molecules are bound simultaneously to P_3^{ago}, maintaining the H-bonds with T279, N280$^{7.45}$, V283, and N284$^{7.49}$. In case of P_2^{ago} and P_3^{ago}, several water molecules compete to bind at the sites (Figs. S6B-C). Along with these trapped waters, the water cluster is observed in the pocket formed by TM1, TM2, TM3, and TM7, especially interacting with N24$^{1.50}$, D52$^{2.50}$, N280$^{7.45}$, and S281$^{7.46}$. These water molecules constitutes an extended allosteric interface between TM helices, helping the receptor activation.

In the antagonist-bound form, trapped water molecules are observed in two sites (Fig. S5C). One (P_1^{antago}) is near the DRY motif, which forms the ionic-lock (i.e., salt-bridge between R102$^{3.50}$ and E228 observed in the inactive state). The water molecules in P_1^{antago} do not form a direct interaction with DRY motif but make a tight H-bonding network with T117 and R120. The residue R120 also makes the H-bonds

with D101 and Y112. The other site P_2^{antago} is identified among the microswitch residues in TM1, TM2, and TM7. The water molecule in this site makes the H-bonds with N24$^{1.50}$, S281$^{7.46}$, and Y288$^{7.53}$, and in the antagonist-bound state, N24$^{1.50}$ interacts with D52$^{2.50}$ in TM2 via H-bonds.

In each receptor state, water molecules help extending interactions of the residues belonging to different TM helices, thus stabilizing the interhelical configurations of GPCRs.

Formation of water wires. A closer look at the movies of water dynamics through the TM domain (SI Movies M1, M2, and M3) reveals the presence of "water wires" in a few locations. Especially in the antagonist-bound inactive state, water molecules are aligned into one dimensional arrays and move in concert, stabilized by the successive H-bonds (5, 6). Macro-dipole moment, $\vec{\mathcal{M}} = \sum_{i=1}^{N} q_i \vec{r}_i$, where i denotes the index of atoms (oxygen or hydrogen) comprising water molecules and N is the total number of atoms, was calculated for the waters in the entire TM domain, and to demonstrate the presence of water wires quantitatively we calculated *regional* macrodipole moment, $\vec{\mathcal{M}}_{\mathcal{R}} = \sum_{i\in\mathcal{R},i=1}^{N_{\mathcal{R}}} q_i \vec{r}_i$ where $N_{\mathcal{R}}$ is the number of atoms composing water molecules in the region $\mathcal{R} = A$, B, or C specified in Figure S5. Excluding the early stage of simulation ($t < 400$ ns) when the water flux is not yet in the steady state, we find that $|\vec{\mathcal{M}}| \approx 20$ Debye and occasionally reaches $|\vec{\mathcal{M}}| > 55$ Debye (Figure S5). In the regions above and below W246$^{6.48}$, where water wires are clearly observed, the regional macrodipole moments are $|\vec{\mathcal{M}}_A| \approx 9.9 \pm 2.6$, $|\vec{\mathcal{M}}_B| \approx 9.8 \pm 2.8$, and $|\vec{\mathcal{M}}_C| \approx 5.7 \pm 2.5$ Debye. It is noteworthy that the orientation of the regional macro-dipole moment of the water wire in the region A is opposite to those in B and C.

SUPPORTING MOVIES

Supporting Movie M1. Water dynamics in the *apo* form during the time interval $t = 1100 - 1150$ ns. All the water oxygens are shown with small spheres in different colors. The key micro-switch residues are depicted using the stick representation marked with their residue numbers.

Supporting Movie M2. Water dynamics in the *agonist*-bound form during the time interval $t = 700 - 750$ ns. The details of the representation are identical with Movie M1.

Supporting Movie M3. Water dynamics in the *antagonist*-bound form during the time interval $t = 700 - 750$ ns. The details of the representation are identical with Movie M1.

Supporting Movie M4. Dynamics of two water molecules in the apo form around the P_2^{apo} for the time interval $t = 821 - 835$ ns. The receptor structure is represented as white ribbon, and two water molecules that compete around P_2^{apo} are depicted using spheres in cyan and green.

References

[1] Li, T., A. A. Hassanali, Y.-T. Kao, D. Zhong, and S. J. Singer, 2007. Hydration dynamics and time scales of coupled water-protein fluctuations. *J. Am. Chem. Soc.* 129:3376–3382.

[2] Wood, K., M. Plazanet, F. Gabel, B. Kessler, D. Oesterhelt, D. Tobias, G. Zaccai, and M. Weik, 2007. Coupling of protein and hydration-water dynamics in biological membranes. *Proc. Natl. Acad. Sci. U. S. A.* 104:18049–18054.

[3] Yoon, J., J.-C. Lin, C. Hyeon, and D. Thirumalai, 2014. Dynamical Transition and Heterogeneous Hydration Dynamics in RNA. *J. Phys. Chem. B* 118:7910–7919.

[4] Fogarty, A. C., and D. Laage, 2014. Water dynamics in protein hydration shells: the molecular origins of the dynamical perturbation. *J. Phys. Chem. B.* 118:7715–7729.

[5] Raghavender, U. S., S. Aravinda, N. Shamala, R. Rai, and P. Balaram, 2009. Characterization of water wires inside hydrophobic tubular peptide structures. *J. Am. Chem. Soc.* 131:15130–15132.

[6] Reddy, G., J. E. Straub, and D. Thirumalai, 2010. Dry amyloid fibril assembly in a yeast prion peptide is mediated by long-lived structures containing water wires. *Proc. Natl. Acad. Sci. U. S. A.* 107:21459–21464.

SUPPORTING FIGURES

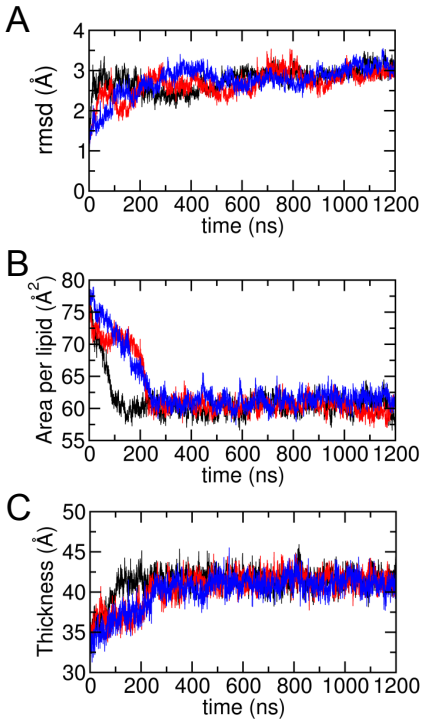

Figure S1: **Protein RMSD and lipid characteristics during the simulations.** (A) RMSD of the protein backbone structures for apo (black), agonist-bound (red), and antagonist-bound (blue) forms. (B) Area per POPC lipid and (C) membrane thickness of bilayers (average distance between phosphorus atoms of POPC lipid in the upper and lower leaflets).

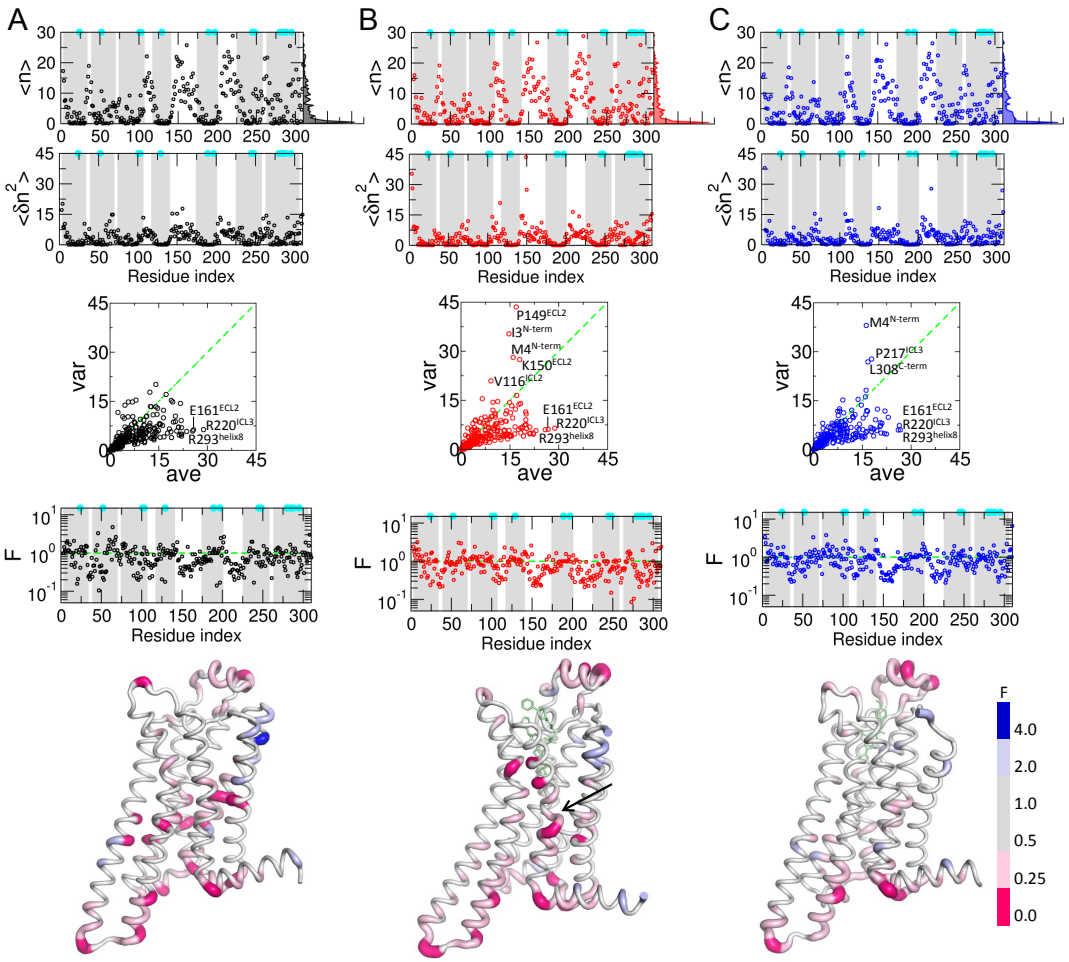

Figure S2: **Number fluctuation of surface water molecules and their Fano factor.** Average ($\langle n \rangle$) and variance ($\langle (\delta n)^2 \rangle$) of water number are calculated around each residue using cut-off distance $R_c = 4$ Å from any heavy atom in the (A) apo, (B) agonist-bound, and (C) antagonist-bound forms. The ratio between the average and variance, i.e., Fano factor, are displayed at the bottom graph. The TM regions are shaded in grey, and the positions of microswitch residues are marked with cyan dots. The histogram of $\langle n \rangle$, $P(\langle n \rangle)$, over the residues are shown on the right hand side of the graph for $\langle n \rangle$. In the scatter plots in the middle, the dashed line corresponds to $F = 1$ ($\langle \delta n^2 \rangle = \langle n \rangle$). The residues with $F \gg 1$ are all found in the loop and terminal regions, and those with $F \ll 1$ and $25 \lesssim \langle n \rangle < 30$ are commonly identified in all the ligand states to be E161, R220, R293 in the ECLs and ICLs. The receptor structures are colored in accord with the F value, and the bound ligands are shown in light-green sticks. The region associated with the water cluster, identified in Fig. 1B, is marked with the arrow.

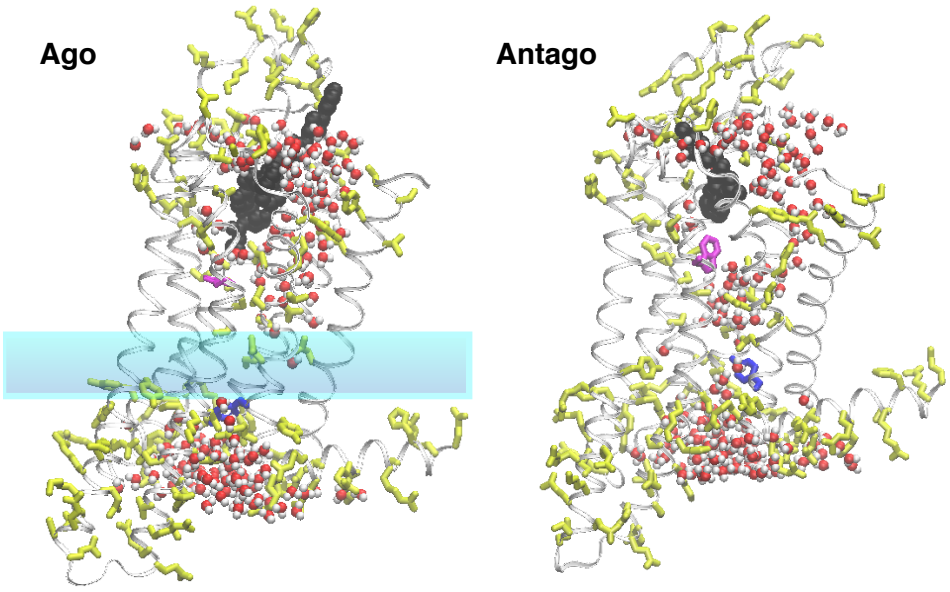

Figure S3: **Water pathways along the alignment of polar residues in the TM domain.** TM domain is made mostly of nonpolar residues (white ribbon). Polar residues, depicted together with their side-chain in yellow sticks, display a characteristic "Y" shaped alignment, which internal water molecules in sphere representation hydrate. The agonist and antagonist ligands are depicted in black spheres, and W246 and Y288 are shown in magenta and blue sticks, respectively. In the agonist-bound form, the water free zone, corresponding to HL2, is highlighed in the middle, whereas in the antagonist-bound form, the water molecules are bridged through the TM channel along the polar residues.

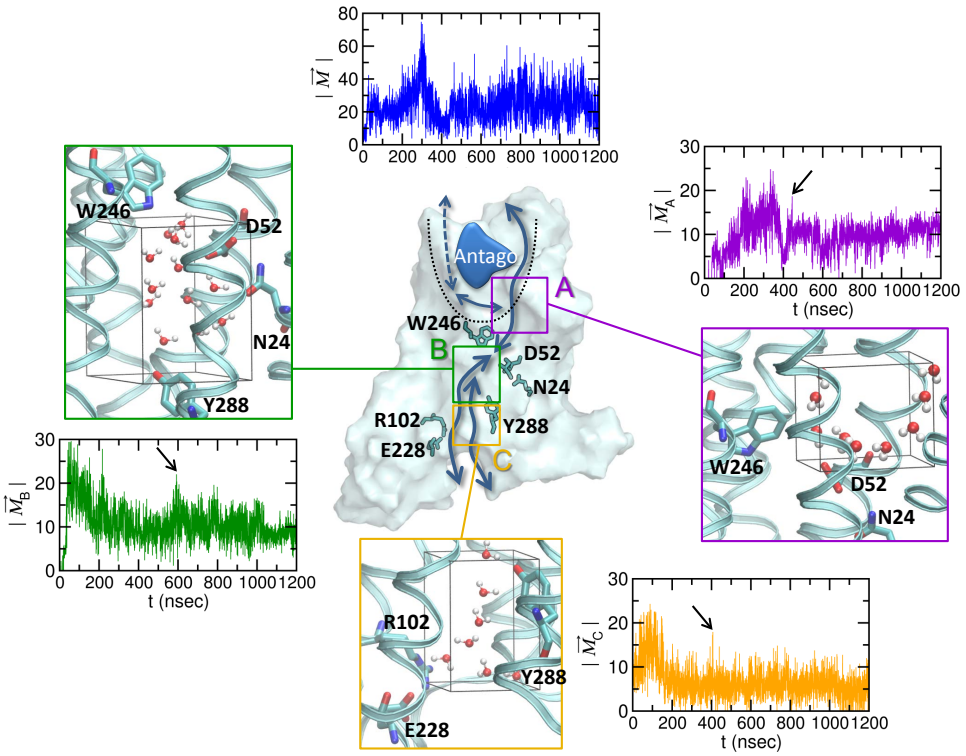

Figure S4: **Water wires.** Macrodipole moment ($|\vec{\mathcal{M}}|$) for the entire population of water in the TM region (blue), and regional macrodipole moments ($|\vec{\mathcal{M}}_{\mathcal{R}}|$ with $\mathcal{R}$ = A, B, and C) calculated for the water in the regions A, B, and C. The snapshots are taken for the water configuration in each region with the maximal regional macrodipole moments (marked with an arrow in each panel) for $t > 400$ ns.

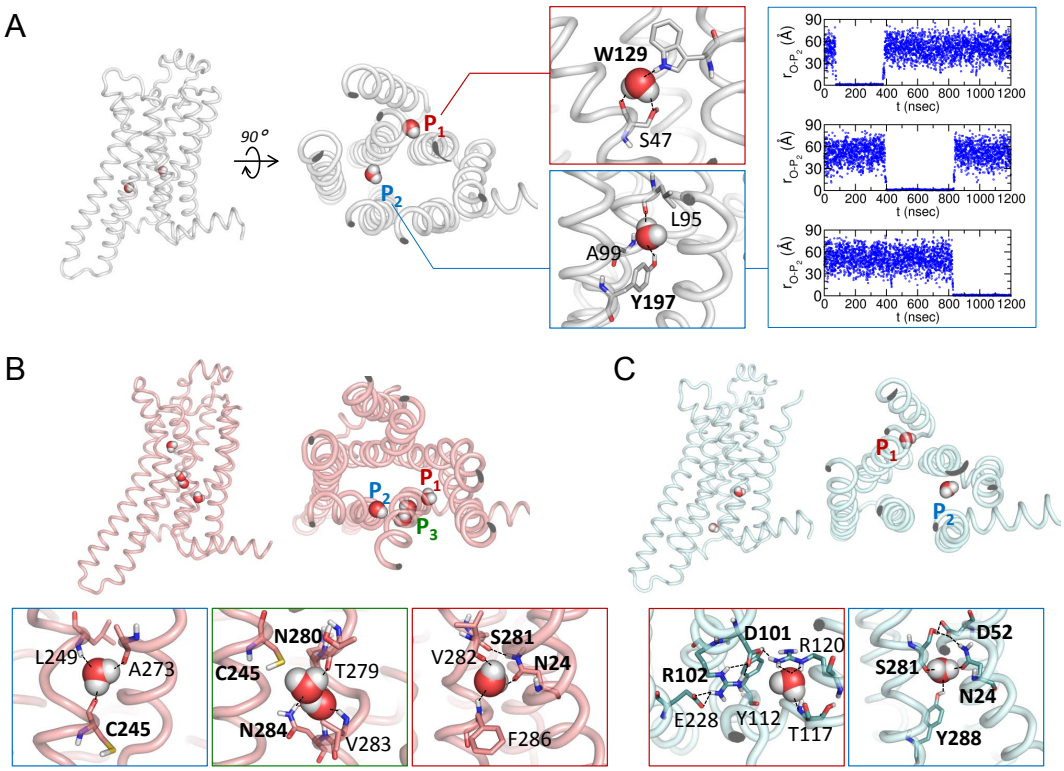

Figure S5: **Trapped water molecules and their interactions with the receptor.** (A) Trapped water molecules in the apo form. The receptor secondary structure is displayed in tube, and the trapped water molecules are depicted in spheres. The H-bonds are represented in black dashed lines, and the interacting residues are annotated. The distances of the three water molecules relative to the site P_2^{apo} are displayed on the right to show the water dynamics (see also Supporting movie M4). (B) Agonist-bound form. (C) Antagonist-bound form. The distances of water molecules from the trapping sites are shown in Fig. S6.

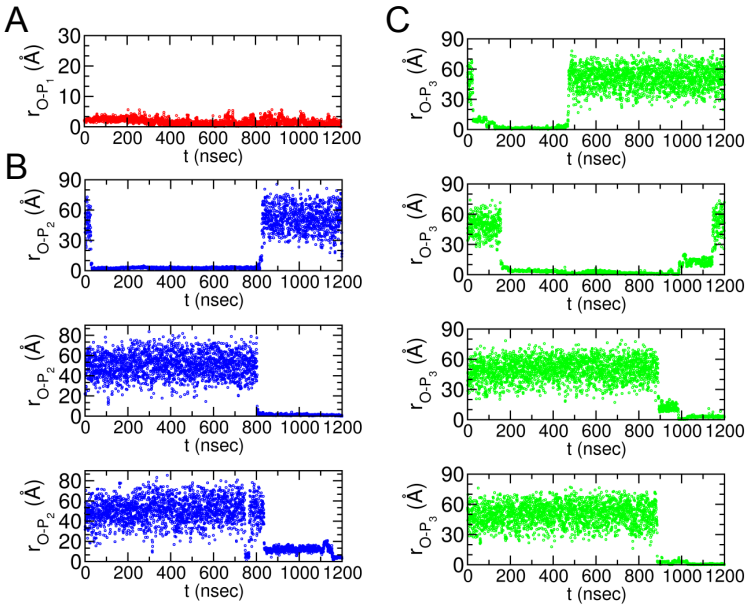

Figure S6: **Dynamics of water trapping is visualized using the distance of a water molecule relative to the site where the water is trapped.** (A) Dynamics of a water trapped in P_1^{apo}. (B) Dynamics of three water molecules trapped in P_2^{ago}. (C) Dynamics of four water molecules trapped in P_3^{ago}.

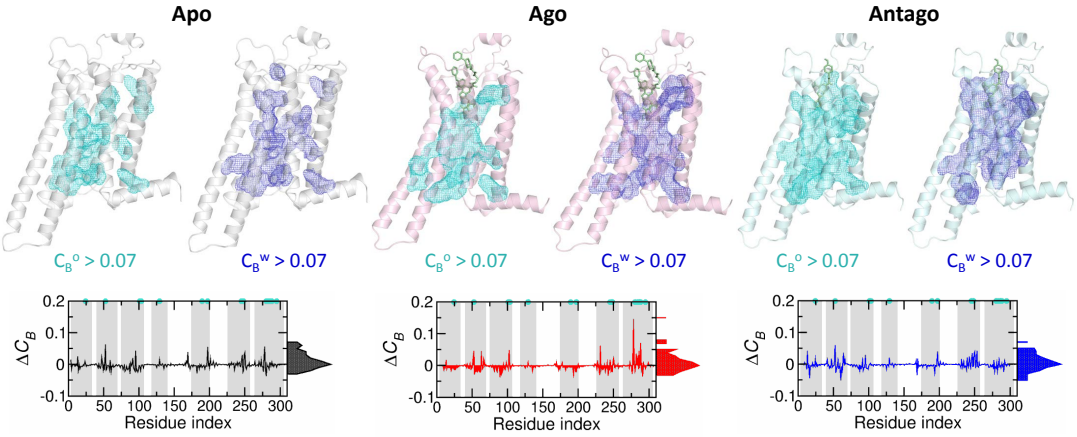

Figure S7: **Analysis of allosteric interface using betweenness centrality.** Betweenness centrality (C_B) were calculated for two residue interaction networks. (i) C_B^o, based on the network that takes into account the residue-residue interaction in direct contact (between any heavy atom in the residues within $R_c \leq 4$ Å), and (ii) C_B^{w}, based on the network that takes into account the water-mediated residue-residue contact in which two residues either shares the same water molecule and satisfies residue-water oxygen distance cut-off value of 3.5 Å or are in direct contact within the distance of 4 Å. Allosteric interface using $C_B^o > 0.07$ and $C_B^{\text{w}} > 0.07$ are shown on the top for each receptor state.